2D FEM CODE WITH THIRD ORDER APPROXIMATION FOR RF CAVITY COMPUTATION

Jacek Sekutowicz
DESY, Notkestraße 85, 22603 Hamburg

ABSTRACT

A 2D Frequency Domain Finite Element Method (FD FEM) code for cylindrically symmetric cavities is presented. Third order approximation of the field function and the approximation of a domain with both straight and curvilinear triangles, allow high accuracy, even for a very sparse mesh. A test of the program and a practical example of rf structure computation are given.

DESCRIPTION OF THE METHOD

For the TM0xx type resonant modes of any cylindrically symmetric structure one can formulate the field problem in a form of the Helmholtz equation. This equation for the angular magnetic field component H_φ (the only component of the magnetic field) is as follows:

$$(\nabla_c^2 + \omega^2\varepsilon\mu)H_\varphi = 0 \qquad (1)$$

where ∇_c^2 is the Laplacian with axial symmetry[1] . Boundary conditions which should be usually fulfilled are: $\mathbf{n}\cdot H_\varphi=0$ and/or $H_\varphi=0$. Using the field function $u= rH_\varphi$ equation (1) and the boundary conditions can be written in the new form:

$$\frac{\partial}{\partial r}\left[\frac{1}{r}\frac{\partial u}{\partial r}\right]+\frac{\partial}{\partial z}\left[\frac{1}{r}\frac{\partial u}{\partial z}\right]+\lambda\frac{u}{r}=0 \qquad (2.1)$$

$$\begin{cases}\dfrac{\partial u}{\partial n}=0 & \text{electric short}\\ u=0 & \text{magnetic short}\end{cases} \qquad (2.2)$$

where $\lambda=\omega^2\varepsilon\mu$.

All field components can be found when u is known:

$$E_r=\frac{1}{i\omega\varepsilon}\cdot\frac{1}{r}\frac{\partial u}{\partial z}\quad,\quad E_z=-\frac{1}{i\omega\varepsilon}\cdot\frac{1}{r}\frac{\partial u}{\partial r}\quad,\quad H_\varphi=\frac{u}{r}.$$

We will look for the solution to the eigenvalue problem (2.1) in Sobolev space $H^1(\Omega,1/r)$:

$$H^1(\Omega,1/r)\equiv\left\{v\in L^2(\Omega,1/r):\frac{\partial v}{\partial r},\frac{\partial v}{\partial z}\in L^2(\Omega,1/r)\right\} \qquad (3)$$

The domain Ω is the axial cross section of the structure, and $L^2(\Omega,1/r)$ is the Hilbert space defined:

$$L^2(\Omega,1/r)\equiv\left\{v:\int_\Omega\frac{v^2}{r}drdz<\infty\right\} \qquad (4)$$

with the inner product:

$$\forall v_1,v_2\in L^2(\Omega,1/r):<v_1,v_2>_{1/r}\equiv\int_\Omega\frac{v_1v_2}{r}drdz \qquad (5)$$

Multiplying (2.1) with a function $v\in H^1(\Omega,1/r)$ and integrating by parts, one obtains a weak formulation of the problem. For each solution $\{\lambda,u\}$ the weak formulation is:

$$A(u,u)-\lambda<u,u>_{1/r}=0 \qquad (6)$$

where A is the bilinear form:

$$A(v_1,v_2)=\int_\Omega\frac{1}{r}\left(\frac{\partial v_1}{\partial r}\frac{\partial v_2}{\partial r}+\frac{\partial v_1}{\partial z}\frac{\partial v_2}{\partial z}\right)drdz \qquad (7)$$

To define the finite dimensional subspace $V_h\subset H^1(\Omega,1/r)$ in which we will look for the numerical solution to (6) one has to divide domain Ω into parts as it is shown in Fig.1. The triangulation results in two triangle types: S_i,with one curvilinear side and T_j with straight sides:

$$\Omega=\bigcup_j T_j\cup\bigcup_i S_i$$

Each triangle is assumed to be a transformation of the standard triangle T_o (Fig.2). The mapping χ_j: $T_o\to T_j$ or χ_i: $T_o\to S_i$ is defined as proposed by M.Zlamal [1]:

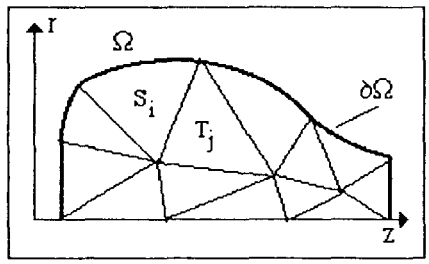

Fig.1 Triangulation of the domain Ω.

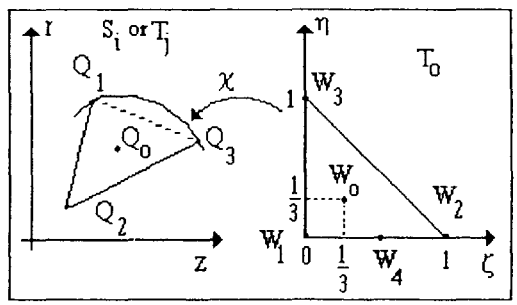

Fig.2 Isoparametric mapping from $T_o\to T_j$ (S_i)

$$\chi_k\equiv\begin{cases}r=r_{k_1}+(r_{k_2}-r_{k_1})\zeta+(r_{k_3}-r_{k_1})\eta+(1-\zeta-\eta)\Phi_k\\ z=z_{k_1}+(z_{k_2}-z_{k_1})\zeta+(z_{k_3}-z_{k_1})\eta+(1-\zeta-\eta)\Psi_k\end{cases} \qquad (8)$$

Here, k is either i or j depending on the triangle type, (r_{kn},z_{kn}) are coordinates of the nodes Q_{kn} n=1..3, and $\zeta,\eta\in[0,1]$. The curvilinear side of each S_i triangle is approximated by a 3rd–order Hermite polynomial. This simplifies Φ_k and Ψ_k:

$$\Phi_k(\eta)=a_k\eta+b_k\eta^2 \qquad (9.1)$$

$$\Psi_k(\eta)=c_k\eta+d_k\eta^2 \qquad (9.2)$$

The coefficients: a_k, b_k, c_k, d_k are given by the parametric description of a curvilinear side: $r=\varphi(s)$, $z=\psi(s)$ for $s\in[s_1,s_3]$:

$$a_k=(s_3-s_1)\frac{d\varphi_k}{ds}(s_1)-r_{k_3}+r_{k_1} \qquad (10.1)$$

$$b_k=2(r_{k_3}-r_{k_1})-(s_3-s_1)\left(\frac{d\varphi_k}{ds}(s_1)+\frac{d\varphi_k}{ds}(s_3)\right) \qquad (10.2)$$

---

[1] Due to the symmetry system of the cylindrical coordinates {r,φ,z} will be used.

$$c_k = (s_3 - s_1)\frac{d\psi_k}{ds}(s_1) - z_{k3} + z_{k1} \qquad (10.3)$$

$$d_k = 2(z_{k3} - z_{k1}) - (s_3 - s_1)\left(\frac{d\psi_k}{ds}(s_1) + \frac{d\psi_k}{ds}(s_3)\right) \qquad (10.4)$$

The approximation of curvilinear sides causes S-type triangles to be approximated by triangles S^* having a new curvilinear side and thus the whole domain Ω is approximated by the new domain Ω^*. Subspace $V_h \subset H^1(\Omega,1/r)$ will be made of functions v_h defined in the following way:

$$v_h(r,z) \equiv v_k(r,z) = \begin{cases} v_j(r,z) & \text{for } (r,z) \in T_j \\ v_i(r,z) & \text{for } (r,z) \in S_i \end{cases} \qquad (11.1)$$

where:

$$v_k(r,z) \equiv (w \circ \chi_k^{-1})(r,z) \qquad (11.2)$$

and w is the 3rd-order polynomial over the triangle T_o:

$$w(\zeta,\eta) = b_1 + b_2\zeta + b_3\eta + b_4\zeta^2 + b_5\zeta\eta + b_6\eta^2 + b_7\zeta^3 + b_8\zeta^2\eta + b_9\zeta\eta^2 + b_{10}\eta^3 \qquad (11.3)$$

Nodes (see Fig.2) and node parameters at T_o have been chosen for determination of the polynomial $w(\zeta,\eta)$:

for triangles with one side on axis:

nodes: $W_1=(0,0)$, $W_2=(1,0)$, $W_3(0,1)$, $W_4(1/2,0)$

parameters: $w(W_n)$ and $\frac{\partial w}{\partial \zeta}(W_n)$ for n=1,2,3

$\frac{\partial w}{\partial \eta}(W_n)$ for n=1,2,3,4

for other triangles:

nodes: $W_1=(0,0)$, $W_2=(1,0)$, $W_3(0,1)$, $W_o(1/3,1/3)$

parameters: $w(W_n)$ for n=0,1,2,3

$\frac{\partial w}{\partial \zeta}(W_n)$, $\frac{\partial w}{\partial \eta}(W_n)$ for n=1,2,3

GENERAL EIGENVALUE PROBLEM

The triangulation yields new expressions for both integrals in (6):

$$\int_{\Omega^*} \frac{1}{r}\left(\left(\frac{\partial v_h}{\partial r}\right)^2 + \left(\frac{\partial v_h}{\partial z}\right)^2\right)drdz = \sum_j \int_{T_j} \frac{1}{r}\left(\left(\frac{\partial v_j}{\partial r}\right)^2 + \left(\frac{\partial v_j}{\partial z}\right)^2\right)drdz + \sum_i \int_{S_i^*} \frac{1}{r}\left(\left(\frac{\partial v_i}{\partial r}\right)^2 + \left(\frac{\partial v_i}{\partial z}\right)^2\right)drdz \qquad (12.1)$$

$$\int_{\Omega^*} \frac{1}{r}(v_h^2)drdz = \sum_j \int_{T_j} \frac{1}{r}(v_j^2)drdz + \sum_i \int_{S_i^*} \frac{1}{r}(v_i^2)drdz \qquad (12.2)$$

The way we choose node parameters and the transformation χ determines for each triangle of the domain Ω vector $\mathbf{v}_h$ and matrices $\mathbf{A}_k$ and $\mathbf{B}_k$ such that:

$$\int_{S^* \text{or} T} \frac{1}{r}\left(\left(\frac{\partial v_k}{\partial r}\right)^2 + \left(\frac{\partial v_k}{\partial z}\right)^2\right)drdz = (\mathbf{v}_h)^T \mathbf{A}_k \mathbf{v}_h \qquad (13.1)$$

$$\int_{S^* \text{or} T} \frac{1}{r}(v_k^2)drdz = (\mathbf{v}_h)^T \mathbf{B}_k \mathbf{v}_h \qquad (13.2)$$

Vector $\mathbf{v}_h$ contains both values of the function v_h and values of its derivatives: $\partial v_h/\partial r$ and $\partial v_h/\partial z$, at points $Q_n=\chi(W_n)$ (see Fig.2). The dimension of the vector, depending on the position of the triangle, is:

10 if triangle does not touch axis,

7 if there is one node on the axis,

3 if triangle has one side on the axis.

The set of linear equations relating $\mathbf{v}_h$ to the coefficients $\mathbf{b}=(b_1, b_2,...)$ is:

$$\mathbf{b} = \mathbf{S}^{-1} \cdot \Lambda_k \cdot \mathbf{v}_h \qquad (14)$$

Matrices S and Λ_k are determined by the position of nodes in T_o and transformation χ, respectively. For example, in case of any triangles with no nodes on axis, S and Λ_k are:

$$S = \begin{bmatrix} \mathbf{q}^T(W_1) \\ \mathbf{q}_\zeta^T(W_1) \\ \mathbf{q}_\eta^T(W_1) \\ \mathbf{q}^T(W_2) \\ \mathbf{q}_\zeta^T(W_2) \\ \mathbf{q}_\eta^T(W_2) \\ \mathbf{q}^T(W_3) \\ \mathbf{q}_\zeta^T(W_3) \\ \mathbf{q}_\eta^T(W_3) \\ \mathbf{q}^T(W_0) \end{bmatrix} \quad \text{where:} \quad \begin{aligned} \mathbf{q}^T &= (1,\zeta,\eta,\zeta^2,\zeta\eta,\eta^2,\zeta^3,\zeta^2\eta,\zeta\eta^2,\eta^3) \\ \mathbf{q}_\zeta^T &= (0,1,0,2\zeta,\eta,0,3\zeta^2,2\zeta\eta,\eta^2,0) \\ \mathbf{q}_\eta^T &= (0,0,1,0,\zeta,2\eta,0,\zeta^2,2\zeta\eta,3\eta^2) \end{aligned}$$

$$\Lambda_k = \begin{bmatrix} 1 & 0 & 0 & 0 & 0 & 0 & 0 & 0 & 0 & 0 \\ 0 & \frac{\partial r}{\partial \zeta}(W_1) & \frac{\partial z}{\partial \zeta}(W_1) & 0 & 0 & 0 & 0 & 0 & 0 & 0 \\ 0 & \frac{\partial r}{\partial \eta}(W_1) & \frac{\partial z}{\partial \eta}(W_1) & 0 & 0 & 0 & 0 & 0 & 0 & 0 \\ 0 & 0 & 0 & 1 & 0 & 0 & 0 & 0 & 0 & 0 \\ 0 & 0 & 0 & 0 & \frac{\partial r}{\partial \zeta}(W_2) & \frac{\partial z}{\partial \zeta}(W_2) & 0 & 0 & 0 & 0 \\ 0 & 0 & 0 & 0 & \frac{\partial r}{\partial \eta}(W_2) & \frac{\partial z}{\partial \eta}(W_2) & 0 & 0 & 0 & 0 \\ 0 & 0 & 0 & 0 & 0 & 0 & 1 & 0 & 0 & 0 \\ 0 & 0 & 0 & 0 & 0 & 0 & 0 & \frac{\partial r}{\partial \zeta}(W_3) & \frac{\partial z}{\partial \zeta}(W_3) & 0 \\ 0 & 0 & 0 & 0 & 0 & 0 & 0 & \frac{\partial r}{\partial \eta}(W_3) & \frac{\partial z}{\partial \eta}(W_3) & 0 \\ 0 & 0 & 0 & 0 & 0 & 0 & 0 & 0 & 0 & 1 \end{bmatrix}$$

Matrices $\mathbf{A}_k$ and $\mathbf{B}_k$ are given by the formulae:

$$\mathbf{A}_k = \Lambda_k^T \cdot \mathbf{S}^{-T} \cdot \mathbf{D}_1 \cdot \mathbf{S}^{-1} \cdot \Lambda_k \qquad (15.1)$$

$$\mathbf{B}_k = \Lambda_k^T \cdot \mathbf{S}^{-T} \cdot \mathbf{D}_2 \cdot \mathbf{S}^{-1} \cdot \Lambda_k \qquad (15.2)$$

where matrices $\mathbf{D}_1$ and $\mathbf{D}_2$ represent integration of products:

$$\mathbf{q}_\zeta \times \mathbf{q}_\zeta^T \quad \mathbf{q}_\zeta \times \mathbf{q}_\eta^T \quad \mathbf{q}_\eta \times \mathbf{q}_\eta^T \quad \mathbf{q} \times \mathbf{q}^T \qquad (16)$$

over T_o, resulting from the change of variables (r,z) to (ζ,η) in both integrals (13.1) and (13.2).

The global numbering of all nodes yields the matrix general eigenvalue problem for the global matrices **A**, **B** and the global vector $\mathbf{V}_h$:

$$(\mathbf{A} - \lambda\mathbf{B}) \cdot \mathbf{V}_h = 0 \qquad (17)$$

The presented method has been programmed in FORTRAN-77 and equipped with a mesh generating subroutine, written especially for this code.

TEST AND EXAMPLE

Two rf cavities: pill-box and spherical, for which solutions to (1) are given by Bessel functions, have been used to estimate convergence of the FEM solution vs. mesh size N (number of unknowns). Fig.3 and 4 present frequency error abs(df/f) vs. N for the lowest frequency modes. Since, the presented code allows the mesh to be sparse, both diagrams contain few results for the manually prepared mesh (FEM MM). Other results have been obtained with a generated mesh (FEM MG). The quality of the solution obtained with the generated mesh seems to be, from the application point of view, the most interesting. Expected eigenvalue (frequency) convergence of the FEM presented here is $O(h^5)$. Since, $h \approx (N)^{1/2}$, frequency should converge as $O(N^{2.5})$. The plotted error is a sum of: a FEM approximation error, an algebraic solver error, a mesh generator error and a numerical integration error (only if S_t triangles are used). In the case of the pill-box cavity convergence is better then $O(N^{2.9})$ for whole range of N. For the spherical cavity convergence is slower due to the numerical integration procedure. Nevertheless, in both cases for N~350 the error is smaller then 10^{-5}. For comparison, URMEL and URMEL-T results are included in both diagrams [2,3].

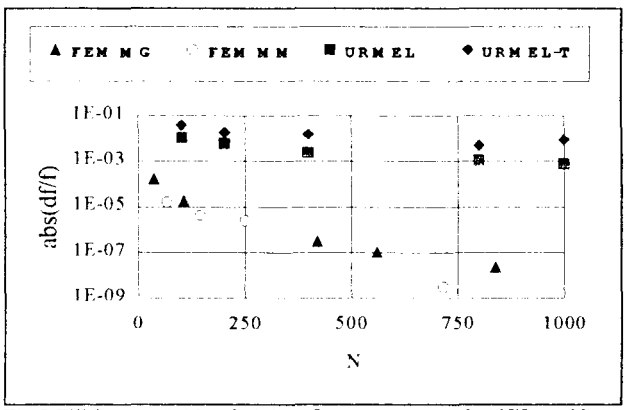

Fig.3 Pill-box (r=0.04m, l=0.1m) frequency error abs(df/f) vs. N.

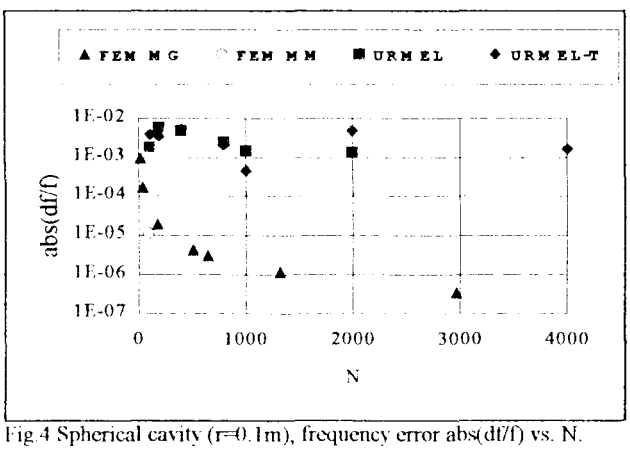

Fig.4 Spherical cavity (r=0.1m), frequency error abs(df/f) vs. N.

In Fig.5 computed parameters of the inner cell of sc TESLA cavity are presented [4]. All FEM results (a,b,c) show regular behavior vs.N. The frequency of the fundamental mode predicted by the FEM code f=1300.9MHz was in agreement with the measured value on all five Cu models of the TESLA structure. The prediction of URMEL was f=1300.1MHz (N=50000/cell) [5]. The change of Epeak/Eacc vs. N computed by the FEM code (c) is smoother due to the 3rd-order approximation of the boundary, as compare to the values found by URMEL (d). The regular field distribution on the metal wall allowed estimation of the frequency change caused by chemical treatment. The computed value of $\Delta f =$ -13KHz/μm has been recently confirmed by the measurement on the Nb prototype. Trajectory computation of multipacting electrons requires well defined fields on the metal wall. Preliminary calculations obtained with new developed code [6] show that using as the input FEM fields, gives more promising results than using as the input fields obtained with codes based on Finite Difference Method.

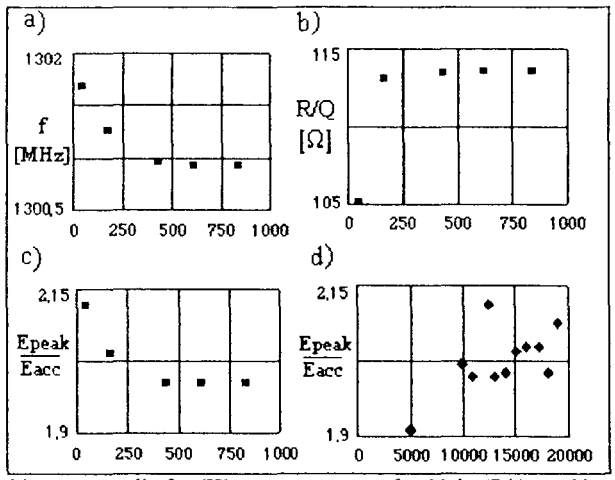

Fig.5 Inner cell of sc TESLA structure. a) f vs.N, b) (R/Q) vs. N, c) Epeak/Eacc vs. N (FEM) d) Epeak/Eacc vs. N (URMEL)

ACKNOWLEDGEMENT

The author is grateful to Dr. S. Kulinski for helpful discussion and to R Brown, C.Henning for help in developing and programming of the Mesh Generator.

REFERENCES

[1] M. Zlamal, "Curved elements in the finite element method" I. SIAM J.Numer. Anal., **10**, 229 (1973), II. SIAM J.Numer. Anal., **11**, 347 (1974).

[2] T. Weiland, "Nuclear Instruments and Methods", **216** , 329, (1983).

[3] U.van Rienen, " Zur numerischen Berechnung zeitharmonischer elektromagnetischer Felder in offenen, zylindersymmetrischen Strukturen unter Verwendung von Mehrgitterverfahren", DESY-Report M-89-04, (1989)

[4] E.Heabel, A.Mosnier, J.Sekutowicz, "Cavity shape optimization for a superconducting linear collider", Procc. of HEACC'92, **II**, 957 (1992).

[5] A.Mosnier, private communication.

[6] C. Stolzenburg , private communication.